型の中でも21種類の一塩基多型（SNP）に焦点を当て、哺乳類細胞発現系を構築して変異タンパク質を発現させ、酵素速度論的解析を行うことによりそれらの変異がXO酵素活性へ与える影響を検証した。

B. 研究方法

すでに作成済みの野生型XOエントリークローンを基にsite-directed mutagenesis法により各々の変異を導入後、哺乳類細胞発現用ベクターに乗せ換えることで変異型XO発現用クローンを得た。21種類の変異型XOは3種類ずつ7回に分け、それぞれ回毎の差の補正のため野生型XOと共にCOS-7細胞により発現させた。野生型及び変異型XOを発現させたCOS-7細胞は、それぞれ回収し、S-9画分を調製した。XOの発現は抗ヒトXO抗体を用いたイムノブロット法により確認した。また、大腸菌発現系を用いて作成したHis-tag融合XOをスタンダードタンパク質として用いそれぞれの変異型XOの発現量の定量を行った。

次に、XOを発現させたCOS-7細胞のS-9画分50 μgを用い、基質であるキサンチンを1.2 μM - 24 μMの濃度範囲でin vitro代謝させ、HPLCにより代謝物である尿酸を定量し、XO酵素活性を算出した。キネティックパラメータはEadie-Hofstee plotを用いて算出し、野生型と変異型XOの酵素機能特性を比較した。

（倫理面への配慮）

今回の研究プロトコールは本邦における「ヒトゲノム・遺伝子解析研究に関する倫理指針」を遵守し、東北薬科大学・大学院倫理委員会および東北大学医学部倫理委員会に申請・承認された同名課題「薬剤反応性遺伝子の多型性が薬効及び薬物動態に与える影響に関する研究」に従って実施された。

C. 研究結果

21種類全ての変異型XOの哺乳類細胞発現用クローンを構築し、変異型XOを発現させることができた。その発現量は、野生型XOと比較しAsn909Lys、Thr910Lys及びPro1150Arg型の変異型において有意な低下が認められた。従って、これらのSNPの存在によるXOの安定性の低下が示唆された。

次に、発現タンパク質の酵素速度論的解析を行った。その結果、21種類の変異型XOのうち、Arg149Cys及びThr910Lys型では酵素活性が検出限界以下、Arg607Gln、Thr623Ile、Asn909Lys及びCys1318Tyr型では酵素活性の有意な低下が認められた。また、His1221Arg型で酵素活性の有意な上昇が認められた。

D. 考察

XO 酵素活性の低下を示す変異では、肝臓での 6-MP 代謝能の低下が予測され、TPMT 酵素活性の低下では説明のできなかった肝機能障害の発症リスクに寄与する可能性が示唆された。XO酵素活性が上昇する変異では、肝臓での6-MP代謝が促進されることが考えられ、6-MP による副作用発現リスクの低下が予想された。その一方、血中へ移行する薬物量の低下が示唆され、ALL 再発リスクの上昇が考えら

れた。

E. 結論

本研究では、6-MPの肝臓での主要代謝酵素であるXO遺伝子多型がXO酵素活性に与える影響を検証し、その結果、酵素活性が変化するXO遺伝子多型の存在を明らかにした。本研究で得られた情報が、これまで未解明であった6-MPによる肝機能障害の発症に関与する因子である可能性が示唆された。今後、これらの情報を、これまでに報告されてきたTPMTの情報と併せて6-MPの投与量設定の際に考慮に入れ、CASSOH法による遺伝子診断法を構築することで、6-MPによる副作用の発現防止やALLの再発防止へ役立つことが期待される。

F. 健康危険情報

G. 研究発表

1. 論文発表

Functional characterization of human xanthine oxidase allelic variants. Mutsumi Kudo, Toshiko Moteki, Takamitsu Sasaki, Yumiko Konno, Shuta Ujiie, Akemi Onose, Michinao Mizugaki, Masaaki Ishikawa, Masahiro Hiratsuka, Pharmacogenet. Genom., 18, 243-251 (2008)

2. 学会発表

なし

H. 知的財産権の出願・登録状況

特になし

厚生労働科学研究費補助金(創薬基盤推進研究事業)

分担研究報告書

日本人集団における有用な薬理遺伝的遺伝子多型情報の収集

分担研究者　平塚　真弘　東北薬科大学講師

研究要旨

近年、ヒトゲノム解析の進展により薬剤反応性の一部が薬物代謝酵素や薬物トランスポーター、薬物受容体遺伝子などのSNPの影響を大きく受けることが明らかにされている。将来的には薬物投与前に薬物動態や薬効発現に関連する遺伝子のSNP診断を行い、患者個々に最適な投与薬剤の選択及び投与量の調整を行うことが可能になる。このようなテーラーメイド医療の展開には、薬剤反応性に影響を及ぼすと考えられる遺伝子をリストアップすることが重要である。今回、日本人集団において、その遺伝子多型が明らかにされていない薬物代謝酵素遺伝子、CYP2J2、CYP2S1及びCYP2W1に関して、Denaturing HPLC(HPLC)を用いたSNPスクリーニングを行った。その結果、CYP2J2ではプロモーターSNPを、CYP2S1及びCYP2W1ではコーディングSNPを同定した。これらの情報は、テーラーメイド医療を推進する上で有益と考えられる。

A. 研究目的

薬物代謝酵素の一つであるチトクローム P450 (cytochrome P450; CYP) は多様な分子種から成る遺伝子スーパーファミリーを構成しており、その中でもCYP2ファミリーには最も多くの分子種が存在している。現在、様々なCYPにおいて、医薬品の薬効や副作用の個人差の原因の一つと考えられている Single nucleotide polymorphism (SNP) の存在が明らかにされている。ヒトの薬物代謝の中心となる臓器には肝臓や小腸があり、多くのCYPは主にこれらの臓器に発現する。しかし近年、主に肝臓以外の組織に特異的に発現している新規CYP2ファミリー分子種が同定された。肝外CYPは、発現組織に特異的な薬物代謝や生体内での内因性基質の生合成あるいは代謝への関与が大きいと考えられている。また、新規分子種であるCYP2J2、CYP2S1及びCYP2W1は各種癌細胞においてその発現が確認されており、これらの発現量が正常組織に比べ癌組織中に高いことや個人差が見られることから癌細胞の機能に何らかの影響を及ぼす可能性が示唆されている。

本研究では、これまで日本人集団において論文報告や遺伝子多型解析がほとんど行われていないCYP2J2、CYP2S1及びCYP2W1遺伝子について、Denaturing high performance liquid chromatography (DHPLC) 法を用いてSNPスクリーニングを行った。またCYP2W1に関しては、得られたSNP情報を基にして、より詳細な遺伝子構造を明らかにする目的でハプロタイプ解析を行った。

B. 研究方法

日本人由来の DNA 200 検体について、CYP2J2 のプロモーター（-3246～+45）とCYP2J2、CYP2S1 及び CYP2W1 の各エキソン（各 9 箇所）について DHPLC 法により SNP スクリーニングを行った。SNP の存在が疑われた検体についてはダイレクトシークエンス解析により塩基配列を確認した。また、CYP2W1 は同一検体で 2 箇所以上の SNP を検出した検体のハプロタイプ解析を行った。ハプロタイプ解析は CYP2W1 遺伝子の全エキソンを含む領域をベクターにライゲーションし、シークエンス解析によりアレルを同定した。

（倫理面への配慮）

今回の研究プロトコールは本邦における「ヒトゲノム・遺伝子解析研究に関する倫理指針」を遵守し、東北薬科大学・大学院倫理委員会および東北大学医学部倫理委員会に申請・承認された同名課題「薬剤反応性遺伝子の多型性が薬効及び薬物動態に与える影響に関する研究」に従って実施された。

C. 研究結果

CYP2J2 遺伝子のプロモーター（-3246～+45）及び全エキソン（9箇所）のSNPスクリーニングの結果、プロモーターにおいて2種の新規SNP（-2104A>G、-587G>A）を検出した。また、既知 SNP として CYP2J2*8（18892G>A; Gly312Arg）、サイレントSNP 2種（183C>T ; Phe61Phe、18919C>A ; Arg321Arg）及びイントロンSNP 3種（10835G>A、16987T>C、18753T>G）を検出した。

次に、CYP2S1遺伝子の全エキソン（9箇所）のSNPスクリーニングの結果、新規アミノ酸置換を伴うSNPである5479T>G（Leu230Arg）が0.25%のアレル頻度で検出された。また、アミノ酸置換を伴わない新規サイレントSNPとして4612G>A（Glu147Glu）及び5478C>T（Leu230Leu）を同定した。白人種において同定されているCYP2S1*2及びCYP2S1*3は、今回解析した日本人検体からは検出されなかったことから、日本人種におけるCYP2S1*2及びCYP2S1*3は存在しないか、あるいは頻度が非常に低いことが示唆された。

CYP2W1遺伝子の全エキソン（9箇所）のSNPスクリーニングの結果、アミノ酸置換を伴う新規SNPとしてCYP2W1のエキソン1（173A>C; Glu58Ala）に1種及びエキソン9（5432G>A; Val432Ile、5584G>C; Gln482His）に2種検出した。またアミノ酸置換を伴う既知SNP 2種（2008G>A; Ala181Thr、5601C>T; Pro488Leu）及びサイレントSNP 1種（166C>T; Leu56Leu）をそれぞれ検出した。さらにハプロタイプ解析を行い、CYP2W1*1B～*6のアレルを同定し、日本人におけるCYP2W1遺伝子が7種類のハプロタイプを含んでいることを明らかにした。アレル頻度を算出した結果、CYP2W1*6 は36.8%と最も高頻度であった。これに対し、野生型アレルCYP2W1*1Aの頻度は29.5%と変異型に比べ低く、日本人におけるCYP2W1遺伝子は変異型を有する割合の方が高いことが明らかになった。

D. 考察

今回焦点を当てたCYP2J2、CYP2S1及びCYP2W1などの肝外CYPは肝臓以外の組織にそれぞれ特異的に発現しており、肝以外での薬物代謝や生体の機能維持等に関わっていると推測されている。CYP2J2については、アラキドン酸代謝に関与し、間接的に心機能や腎機能の調節を行っている可能性があり、血圧や心血管系の疾患との関連性が示唆される。また、CYP2S1やCYP2W1においては癌細胞内での発現についても研究が進められている。これら3種の肝外CYPの関与が予測される高血圧や癌は、環境的要因や数種の遺伝的要因が関与する多因子性疾患である。疾患に関与する可能性がある一つ一つの遺伝子について多型を調べ、その情報を集積することにより、発症リスクの予見や疾患感受性遺伝子の同定に役立つ遺伝マーカーとしての利用が期待される。

E. 結論

今回、遺伝子多型診断によるテーラーメイド医療の実現化を図るべく、日本人集団に特徴的な薬物代謝酵素遺伝子多型の解析を行った。その結果、CYP2J2、CYP2S1及びCYP2W1の遺伝子上に新規SNPが同定された。特に、CYP2W1に関しては多様なバリアントアレルが存在することが明らかになった。

F. 健康危険情報

G. 研究発表

1. 論文発表

Three novel single nucleotide polymorphisms (SNPs) of CYP2S1 gene in Japanese individuals. Yoshiyuki Hanzawa, Takamitsu Sasaki, Masahiro Hiratsuka, Masaaki Ishikawa, Michinao Mizugaki, Drug Metabol. Pharmacokin., 22, 136-140 (2007)

Genetic polymorphisms and haplotype structures of the human CYP2W1 gene in a Japanese population. Yoshiyuki Hanzawa, Takamitsu Sasaki, Michinao Mizugaki, Masaaki Ishikawa, Masahiro Hiratsuka, Drug Metab. Dispos., 36, 349-352 (2008)

2. 学会発表

Genetic Polymorphisms and Haplotype structures of the CYP2W1 Gene in a Japanese Population, Masahiro Hiratsuka, Yoshiyuki Hanzawa, Takamitsu Sasaki, Kanako Sakuyama, Masaaki Ishikawa, Michinao Mizugaki, Maria Karlgren, Masaya Tachibana, Alvin Gomez, Magnus Ingelman-Sundberg, 8th Internatinal ISSX Meeting, Sendai, Japan, October 9-12, 2007

H. 知的財産権の出願・登録状況

特になし

Ⅲ. 研究成果の刊行に関する一覧表

別紙４

研究成果の刊行に関する一覧表

書籍

著者氏名	論文タイトル名	書籍全体の編集者名	書　籍　名	出版社名	出版地	出版年	ページ

雑誌

発表者氏名	論文タイトル名	発表誌名	巻号	ページ	出版年
Hanzawa Y, Sasaki T, Hiratsuka M, Mizugaki M, et al.	Three novel single nucleotide polymorphisms (SNPs) of CYP2S1 gene in Japanese individuals	Drug Metab. Pharmacokinet.	22	136-140	2007
Oda M Kure S, et al.	Direct correlation between ischemic injury and extracellular glycine concentration in mice with genetically altered of the glycine cleavage multienzyme system.	Stroke	38	2157-64	2007
Kanno J, Kure S, et al.	Allelic and non-allelic heterogeneity in pyridoxine dependent seizures revealed by mutational analysis of ALDH7A1 gene.	Mol Genet Metabol	91	384-9	2007
Makita Y, Kure S, Matsubara Y, et al.	Leukemia in Cardio-facio-cutaneous (CFC) syndrome: a patient with a germline mutation in BRAF proto-oncogene	J Pediatr Hematol Oncol	29	287-90	2007
Kanno J, Kure S, et al.	Genomic deletion within GLDC is a major cause of nonketotic hyperglycinemia.	J Med Genet	44	e69	2007
Nava C, Matsubara Y., et al.	Cardio-facio-cutaneous and Noonan syndromes due to mutations in the RAS/MAPK signalling pathway: genotype-phenotype relationships and overlap with Costello syndrome	J Med Genet	44	763-71	2007

Narumi Y, Kure S, Matsubara Y, et al.	Molecular and clinical characterization of cardio-facio-cutaneous (CFC) syndrome: overlapping clinical manifestations with Costello syndrome	Am J Med Genet A	143	799-807	2007
Sakamoto O, Matsubara Y, et al.	Mutation and haplotype analyses of the MUT gene in Japanese patients with methylmalonic acidemia.	J Hum Genet	52	48-55	2007
Kudo M, Sasaki T, Mizugaki M, Hiratsuka M, et al.	Functional characterizationof human xanthine oxidase allelic variants	Pharmacogenet. Genom.	18	243-251	2008
Hanzawa Y, Sasaki T, Mizugaki M, Hiratsuka M, et al.	Genetic polymorphisms and haplotype structures of the human CYP2W1 genein a Japanese population	Drug Metab. Dispos.	36	349-352	2008
松原洋一	存亡の危機に瀕する稀少遺伝性疾患の遺伝子検査	医学のあゆみ			印刷中

Ⅳ. 研究成果の刊行物・別刷

Drug Metab. Pharmacokinet. 22 (2): *SNP29* (136)–*SNP33* (140) (2007).

SNP Communication

Three Novel Single Nucleotide Polymorphisms (SNPs) of CYP2S1 Gene in Japanese Individuals

Yoshiyuki HANZAWA[1,2], Takamitsu SASAKI[1,2], Masahiro HIRATSUKA[1,2], Masaaki ISHIKAWA[2] and Michinao MIZUGAKI[1,*]

[1]*Department of Clinical Pharmaceutics, Tohoku Pharmaceutical University, Sendai, Japan*
[2]*Department of Clinical Pharmacotherapeutics, Tohoku Pharmaceutical University, Sendai, Japan*

Full text of this paper is available at http://www.jstage.jst.go.jp/browse/dmpk

Summary: We analyzed all nine exons and exon-intron junctions of the *CYP2S1* gene in 200 Japanese individuals and identified the following three novel single nucleotide polymorphisms (SNPs): 4612G>A (Glu147Glu) in exon 3, 5478C>T (Leu230Leu) and 5479T>G (Leu230Arg, *CYP2S1*5A*) in exon 5. The allele frequencies were 0.013 for 4612G>A, 0.058 for 5478C>T, and 0.003 for 5479T>G. In addition, a known SNP 1324C>G (Pro74Pro) was detected at a frequency of 0.300.

Key words: CYP2S1; genetic polymorphism; SNP

Introduction

The cytochrome P450s (CYPs) constitute a large and complex gene superfamily. Currently, 57 active *CYP* genes and 58 pseudogenes are known to present in the human genome. Most of the *CYP* genes have the highest expression in the liver, which plays a dominant role in the clearance of foreign compounds. CYP enzymes also metabolize many endogenous compounds important for the maintenance of cellular homeostasis, such as steroids, retinoids, bile acids, fatty acids, and eicosanoids.

Recently, a novel *CYP* gene, *CYP2S1*, has been identified. The *CYP2S1* gene is localized in the *CYP2* gene cluster on chromosome 19q.13.2. Several studies that investigated the tissue distribution of human CYP2S1 mRNA demonstrated that it has low expression levels in the liver but is detectable in extrahepatic tissues such as those of the respiratory and digestive systems.[1-3] Furthermore, CYP2S1 mRNA and protein were detected in human skin, where CYP2S1 was shown to be induced by ultraviolet radiation, coal tar, and *all-trans* retinoic acid.[3,4] In the same study, CYP2S1 was observed to metabolize *all-trans* retinoic acid, indicating that CYP2S1 may be involved in the biotransformation of endogenous substrates important for cell proliferation and differentiation.[5]

The human *CYP2S1* gene has recently been shown to be polymorphic; two amino acid-changing allelic variants *CYP2S1*2* (10347C>T; 13255A>G) and *CYP2S1*3* (13106C>T; 13255A>G) have been detected in Caucasians.[6] *CYP2S1* has been genetically analyzed in Caucasians but not in Japanese individuals. In the present study, nine exons and exon-intron junctions of the *CYP2S1* gene from 200 Japanese individuals were screened for genetic polymorphisms by using denaturing HPLC (DHPLC). We identified three novel single nucleotide polymorphisms of the *CYP2S1* gene, including a nonsynonymous polymorphism, in Japanese individuals.

Materials and Methods

Venous blood was obtained from 200 unrelated healthy Japanese volunteers and patients admitted to Tohoku University Hospital. Written informed consent was obtained from all the blood donors, and the study was approved by the Local Ethics Committee of Tohoku University Hospital and Tohoku Pharmaceuti-

As of December 1, 2006, these SNPs were not found in dbSNP in the National Center for Biotechnology Information (http://www.ncbi.nlm.nih.gov/SNP/), GeneSNPs at the Utah Genome Center (http://www.genome.utah.edu/genesnps/) or the Human CYP Allele Nomenclature Committee database (http://www.imm.ki.se/CYPalleles/). The *CYP2S1* haplotype with 5479T>G (Leu230Arg) was assigned as *CYP2S1*5A* by the Human CYP Allele Nomenclature Committee (http://www.imm.ki.se/CYPalleles/).

Received; December 19, 2006, Accepted; February 13, 2007
**To whom correspondence should be addressed*: Michinao MIZUGAKI, *Department of Clinical Pharmaceutics, Tohoku Pharmaceutical University, 4-4-1, Komatsushima, Aoba-ku, Sendai 981-8558, Japan. Tel. +81-22-727-0211, Fax. +81-727-0149, E-mail: mizugaki@tohoku-pharm.ac.jp*

Table 1. Amplification and DHPLC conditions for *CYP2S1* SNP analysis of genomic DNA

Exon	Size (bp)	Forward primer (5′ to 3′)	Reverse primer (5′ to 3′)	Annealing Temp. (°C)	PCR cycles	DHPLC Temp. (°C)
1	247	gccgcgcggagcgcctggga	ccaggacgtccccagagccc	Slowdown[a] 70.0–55.0	63	65.8, 68.5
2	376	cttggatcgaagaggtcacagc	ttgggatttcaggcactagcc	60.0	35	64.3
3	303	caacagagcgagattccgtctc	agttttccctttcactcggctg	65.0	35	62.9
4	367	ctctctccctgcgctgtcc	gagaagggcagctagttctcatgg	60.0	35	62.6
5	257	tcccatgagaactagctgcc	caccatgcccattcagagag	60.0	30	64.7
6	336	taacttgtgtttccgaccccag	ctcagcctcccaaagtgctg	65.0	35	59.2
7	436	acaagatgtgtggtctttgggc	agaaaaagtcagggagacactgacag	60.0	35	63.0
8	485	tctctcacctcagcctcccac	tcagtattcctcacacccaggc	60.0	35	60.5
9	342	tgaggaatactgactcagccctctc	acactctggagacattaaccctgtcc	60.0	35	62.4

[a]Slowdown protocol: The annealing temperature was decreased after cycle 3 by 1.0°C every 3 cycles, beginning at 70°C and decreased to a "slowdown" annealing temperature of 55°C, followed by 15 additional cycles with an annealing temperature of 60°C. The PCR was used at a ramp rate of 2.5°C/s and reached annealing temperature at 1.5°C/s.

cal University. DNA was isolated from K_2EDTA-anticoagulated peripheral blood by using QIAamp DNA Mini Kits (Qiagen, Hilden, Germany) according to the manufacturer's instructions.

Table 1 lists the primer pairs used to amplify nine exons and exon-intron junctions of the *CYP2S1* gene. These primers were designed based on the genomic sequence reported in GenBank (NG_000008.7). The amplicons for exon 1 were generated using AmpliTaq Gold PCR Master Mix (Applied Biosystems, Foster City, CA, USA). PCR reactions were performed using an iCycler (Bio-Rad, Hercules, CA, USA). Moreover, the method relied on a combination of the slowdown method and the addition of betaine (Sigma-Aldrich, St.Louis, MO) for this region with high GC content (>70%).[7] The PCR condition comprised denaturation at 95°C for 5 minutes, followed by 48 cycles of denaturation at 95°C for 30 seconds, annealing for 30 seconds, extension at 72°C for 40 seconds, and finally, 15 additional cycles at an annealing temperature of 60°C. The amplicons for each exon from 2 to 9 were generated using the AmpliTaq Gold PCR Master Mix. The PCR conditions comprised denaturation at 95°C for 10 minutes, followed by 30 or 35 cycles of denaturation at 95°C for 30 seconds, annealing for 30 seconds, extension at 72°C for 30 seconds, and a final extension at 72°C for 7 minutes. The annealing temperatures and PCR cycles for the screening of *CYP2S1* variants are summarized in **Table 1**. Heteroduplexes were generated by performing thermal cycling as follows: 95°C for 1 minute, followed by a reduction in temperature from 95°C by 45 increments of 1.5°C per minute.

The PCR products were analyzed using the DHPLC system (WAVE®; Transgenomic Inc., Omaha, NE, USA).[8-12] Amplified PCR samples (5 μL) were separated on a heated C18 reverse-phase column (DNAsep®) by using 0.1 M triethylammonium acetate (TEAA) in water and 0.1 M TEAA in 25% acetonitrile at a flow rate of 0.9 mL/min. The software provided with the instrument selected the temperature for the heteroduplex separation of a heterozygous *CYP2S1* fragment. **Table 1** summarizes the DHPLC running conditions for each amplicon. The linear acetonitrile gradient was adjusted to the retention time of the DNA peak at 4–5 minutes. Homozygous nucleotide exchanges can occasionally be detected due to a slight shift in the elution time as compared with that of the reference. The addition of an approximately equal amount of wild-type DNA to the samples (1:1) at the denaturation step enabled the reliable detection of homozygous alterations in exon 2. This was performed for all samples in order to identify homozygous sequence variations. Therefore, all samples were analyzed as follows. First, equal amounts of four samples were mixed to identify the heterozygotes, and then, each sample was mixed with wild-type DNA to detect the homozygous variants. The resultant chromatograms were compared with those of the wild-type DNA.

Both strands of samples in which variants were detected by DHPLC were analyzed using a CEQ8000® automated DNA sequencer (Beckman-Coulter Inc., Fullerton, CA, USA). Further, we sequenced all samples having chromatographic findings that differed from that of the wild-type to establish links between mutations and specific profiles. We sequenced the PCR products by fluorescent dideoxy termination using a DTCS DNA Sequencing Kit (Beckman-Coulter Inc.) according to the manufacturer's instructions.

Table 2. The location of SNPs and frequencies of the *CYP2S1* gene in 200 DNA samples of Japanese individuals

Location	Variant	Amino acid change	SNP ID dbSNP (NCBI)	The number of each genotype	Observed Frequency (%) (95% CI)	Frequency (%) predicted by Hardy-Weinberg law
Exon 2	1324C>G	Pro74Pro	rs338599	C/C: 99	49.5 (42.6–56.4)	49.0
				C/G: 82	41.0 (34.2–47.8)	42.0
				G/G: 19	9.5 (5.4–13.6)	9.0
Exon 3	4612G>A	Glu147Glu	—	G/G: 195	97.5 (95.3–99.7)	97.5
				G/A: 5	2.5 (0.3–4.7)	2.5
				A/A: 0	0.0 (0.0)	0.0
Exon 5	5478C>T	Leu230Leu	—	C/C: 177	88.5 (84.1–92.5)	88.8
				C/T: 23	11.5 (7.1–15.9)	10.8
				T/T: 0	0.0 (0.0)	0.3
Exon 5	5479T>G	Leu230Arg	—	T/T: 199	99.5 (98.5–100)	99.5
				T/G: 1	0.5 (0–1.5)	0.5
				G/G: 0	0.0 (0.0)	0.0

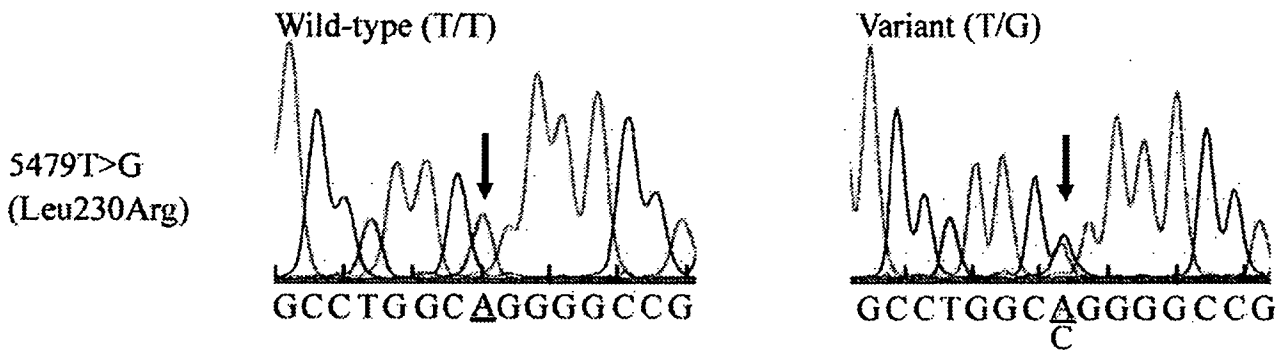

Fig. 1. The nucleotide sequences of the *CYP2S1* gene in exon 5.
Although sequences are shown for anti-sense strands, both strands were sequenced. Arrows indicate the positions of the variant nucleotide.

Results and Discussion

We found the following three novel SNPs:

1) SNP: 061023Hiratsuka10; GENE NAME: *CYP2S1*;
ACCESSION NUMBER: NG_000008; LENGTH: 25 bases;
5′-AGAAGGCGAGGAG/ACTGATCCAGGCG-3′.
2) SNP: 061023Hiratsuka11; GENE NAME: *CYP2S1*;
ACCESSION NUMBER: NG_000008; LENGTH: 25 bases;
5′-TTCCTGCGGCCCC/TTGCCAGGCCCCC-3′.
3) SNP: 061023Hiratsuka12; GENE NAME: *CYP2S1*;
ACCESSION NUMBER: NG_000008; LENGTH: 25 bases;
5′-TCCTGCGGCCCCT/GGCCAGGCCCCCA-3′.

DHPLC analysis of the *CYP2S1* gene in the 200 DNA samples obtained from Japanese individuals revealed chromatographic profiles that were distinct from that of the wild-type in exons 2, 3, and 5. We tested the specificity of DHPLC in detecting the variant allele in these exons by comparing the results with those of direct sequencing. Four SNPs including three novel and one known SNP (rs338599) were detected (**Table 2**). The electrophoretograms of the novel nonsynonymous SNP are shown in **Fig. 1**. The SNP in exon 5 was 5479T>G and resulted in an amino acid change of Leu230Arg. Among the 200 individuals, one was heterozygous for the 5479T>G SNP, suggesting that the allele frequency was 0.003 in the Japanese population. The other novel SNPs 4612G>A and 5478C>T were detected at frequencies of 0.013 and 0.058, respectively. The sequences for each sample were obtained from at least two different PCR amplifications.

The novel SNP 5479T>G is located in exon 5 of the *CYP2S1* gene and results in an amino acid substitution. Homology modeling of the human CYP2 family enzymes based on the CYP2C5 crystal structure lead to speculation that Leu230 is located at the start of the

G-helix.[13,14] In the CYP2 family, this region is not a putative active site.[15,16] However, the Pro227 substitution of CYP2C19 (*CYP2C19*10*) in the same region has been clearly identified as being responsible for the decreased catalytic activity toward *S*-mephenytoin.[17] Pro220 was also one of several critical amino acids that appear to determine the extent of the specificity of CYP2C19 for *S*-mephenytoin as compared to that of CYP2C9.[18] Therefore, the start of the G-helix and F-G loop of the CYP2 family, including CYP2S1, might be associated with enzyme activity.

Numerous genetic polymorphisms have been identified in most *CYP* genes. In particular, genetic polymorphisms of the *CYP2* family are believed to be responsible for large individual variations. Saarikoski *et al.* have detected two variant alleles *CYP2S1*2* and *CYP2S1*3* in the *CYP2S1* gene in the Caucasian population.[6] In the present study we identified the novel variant allele *CYP2S1*5A* in the Japanese population. CYP2S1 could be involved in the metabolism of *all-trans* retinoic acid, which is used to treat skin diseases. CYP2S1 expression was induced in some individuals treated topically with *all-trans* retinoic acid, whereas others showed no response.[3] At least in part, such variation may be caused by sequence variations affecting expression or activity of CYP2S1. However, Wu *et al.* recently reported that CYP2S1 did not catalyze the oxidation of *all-trans* retinoic acid at measurable rate. Further studies on this point are being conducted in our laboratory.

In conclusion, we identified three novel SNPs in the *CYP2S1* gene, including a nonsynonymous polymorphism in Japanese individuals. The nonsynonymous SNP was 5479T>G in exon 5, and it resulted in an amino acid change of Leu230Arg. This SNP has been assigned as *CYP2S1*5A*.

Acknowledgements: This work was supported partly by a Grant-in-Aid for Research on Advanced Medical Technology from the Ministry of Health, Labor and Welfare of Japan and in part by High-Tech Research Center Program from the Ministry of Education, Culture, Sports, Science, and Technology of Japan.

References

1) Rylander, T., Neve, E. P., Ingelman-Sundberg, M. and Oscarson, M.: Identification and tissue distribution of the novel human cytochrome P450 2S1 (CYP2S1). *Biochem. Biophys. Res. Commun.*, **281**: 529-535 (2001).
2) Choudhary, D., Jansson, I., Stoilov, I., Sarfarazi, M. and Schenkman, J. B.: Expression patterns of mouse and human CYP orthologs (families 1-4) during development and in different adult tissues. *Arch. Biochem. Biophys.*, **436**: 50-61 (2005).
3) Smith, G., Wolf, C. R., Deeni, Y. Y., Dawe, R. S., Evans, A. T., Comrie, M. M. Ferguson, J. and Ibbotson, S. H.: Cutaneous expression of cytochrome P450 CYP2S1: individuality in regulation by therapeutic agents for psoriasis and other skin diseases. *Lancet.*, **361**: 1336-1343 (2003).
4) Guengerich, F. P., Wu, Z. L. and Bartleson, C. J.: Function of human cytochrome P450s: characterization of the orphans. *Biochem. Biophys. Res. Commun.*, **338**: 465-469 (2005).
5) Saarikoski, S. T., Rivera, S. P., Hankinson, O. and Husgafvel-Pursiainen, K.: CYP2S1: A short review. *Toxicol. Appl. Pharmacol.*, **207**: 62-69 (2005).
6) Saarikoski, S. T., Suitiala, T., Holmila, R., Impivaara, O., Jarvisalo, J., Hirvonen, A. and Husgafvel-Pursiainen, K.: Identification of genetic polymorphisms of CYP2S1 in a Finnish Caucasian population. *Mutat. Res.*, **554**: 267-77 (2004).
7) Bachmann, H. S., Siffert, W. and Frey, U. H.: Successful amplification of extremely GC-rich promoter regions using a novel 'slowdown PCR' technique. *Pharmacogenetics*, **13**: 759-766 (2003).
8) Hiratsuka, M., Nozawa, H., Konno, Y., Saito, T., Konno, S. and Mizugaki, M.: Human CYP4B1 gene in the Japanese population analyzed by denaturing HPLC. *Drug. Metab. Pharmacokinet.*, **19**: 114-119 (2004).
9) Ebisawa, A., Hiratsuka, M., Sakuyama, K., Konno, Y., Sasaki, T. and Mizugaki, M.: Two novel single nucleotide polymorphisms (SNPs) of the CYP2D6 gene in Japanese individuals. *Drug. Metab. Pharmacokinet.*, **20**: 294-299 (2005).
10) Hiratsuka, M., Kudo, M., Koseki, N., Ujiie, S., Sugawara, M., Suzuki, R., Sasaki, T., Konno, Y. and Mizugaki, M.: A novel single nucleotide polymorphism of the human methylenetetrahydrofolate reductase gene in Japanese individuals. *Drug. Metab. Pharmacokinet.*, **20**: 387-390 (2005).
11) Hiratsuka, M., Nozawa, H., Katsumoto, Y., Moteki, T., Sasaki, T., Konno, Y. and Mizugaki, M.: Genetic polymorphisms and haplotype structures of the CYP4A22 gene in a Japanese population. *Mutat. Res.*, **599**: 98-104 (2006).
12) Sasaki, T., Goto, E., Konno, Y., Hiratsuka, M. and Mizugaki, M.: Three novel single nucleotide polymorphisms of the human thiopurine *S*-methyltransferase gene in Japanese individuals. *Drug. Metab. Pharmacokinet.*, **21**: 332-336 (2006).
13) Lewis, D. F.: Homology modelling of human CYP2 family enzymes based on the CYP2C5 crystal structure. *Xenobiotica*, **32**: 305-323 (2002).
14) Johnson, E. F.: The 2002 Bernard B. Brodie Award lecture: Deciphering substrate recognition by drug-metabolizing cytochromes P450. *Drug Metab. Dispos.*, **31**: 1532-1540 (2003).
15) Lewis, D. F.: The *CYP2* family: models, mutants and interactions. *Xenobiotica*, **28**: 617-661 (1998).
16) Gotoh, O.: Substrate recognition sites in cytochrome P450 family 2 (CYP2) proteins inferred from comparative analyses of amino acid and coding nucleotide sequences. *J. Biol. Chem.*, **267**: 83-90 (1992).
17) Blaisdell, J., Mohrenweiser, H., Jackson, J., Ferguson, S., Coulter, S., Chanas, B., Xi, T., Ghanayem, B. and Goldstein, J. A.: Identification and functional charac-

terization of new potentially defective alleles of human CYP2C19. *Pharmacogenetics*, **12**: 703–711 (2002).
18) Tsao, C. C., Wester, M. R., Ghanayem, B., Coulter, S. J., Chanas, B., Johnson, E. F. and Goldstein, J. A.: Identification of human CYP2C19 residues that confer S-mephenytoin 4′-hydroxylation activity to CYP2C9. *Biochemistry*, **40**: 1937–1944 (2001).

Direct Correlation Between Ischemic Injury and Extracellular Glycine Concentration in Mice With Genetically Altered Activities of the Glycine Cleavage Multienzyme System

Masaya Oda, MD; Shigeo Kure, MD; Taku Sugawara, MD; Suguru Yamaguchi, MD; Kanako Kojima, MD; Toshikatsu Shinka, MD; Kenichi Sato, MD; Ayumi Narisawa, MD; Yoko Aoki, MD; Yoichi Matsubara, MD; Tomoya Omae, MD; Kazuo Mizoi, MD; Hiroyuki Kinouchi, MD

Background and Purpose—Ischemia elicits the rapid release of various amino acid neurotransmitters. A glutamate surge activates *N*-methyl-D-aspartate (NMDA) glutamate receptors, triggering deleterious processes in neurons. Although glycine is a coagonist of the NMDA receptor, the effect of extracellular glycine concentration on ischemic injury remains controversial. To approach this issue, we examined ischemic injury in mice with genetically altered activities of the glycine cleavage multienzyme system (GCS), which plays a fundamental role in maintaining extracellular glycine concentration.

Methods—A mouse line with increased GCS activity (340% of C57BL/6 control mice) was generated by transgenic expression of glycine decarboxylase, a key GCS component (high-GCS mice). Another mouse line with reduced GCS activity (29% of controls) was established by transgenic expression of a dominant-negative mutant of glycine decarboxylase (low-GCS mice). We examined neuronal injury after transient occlusion of the middle cerebral artery in these mice by measuring extracellular amino acid concentrations in microdialysates.

Results—High-GCS and low-GCS mice had significantly lower and higher basal concentrations of extracellular glycine than did controls, respectively. In low-GCS mice, the extracellular glycine concentration reached 2-fold of control levels during ischemia, and infarct volume was significantly increased by 69% with respect to controls. In contrast, high-GCS mice had a significantly smaller infarct volume (by 21%). No significant difference was observed in extracellular glutamate concentrations throughout the experiments. An antagonist for the NMDA glycine site, SM-31900, attenuated infarct size, suggesting that glycine operated via the NMDA receptor.

Conclusions—There is a direct correlation between ischemic injury and extracellular glycine concentration maintained by the GCS. (***Stroke.* 2007;38:2157-2164.**)

Key Words: animal models ■ glutamate ■ glycine ■ neuroprotection ■ NMDA glutamate receptor ■ reperfusion ■ transgenic mice

An abnormal increase in extracellular glycine concentration, together with a rapid elevation of glutamate, is consistently elicited by ischemia.[1] The elevation of glutamate leads to uncontrolled activation of *N*-methyl-D-aspartate (NMDA) receptors and intracellular penetration of calcium, which is followed by production of free radicals, mitochondrial dysfunction, DNA injury, and deleterious processes that finally lead to the demise of surrounding neurons.[2] Activation of NMDA receptors is therefore considered a key process in the development of ischemic injury. Glycine is an inhibitory neurotransmitter in the brain stem and spinal cord,[3] and it also plays a critical role as a modulator of NMDA receptors.[2,4] The role of glycine in stroke remains controversial. In acutely prepared hippocampal slices, excitotoxicity and subsequent neuronal cell death could be induced by addition of high concentrations of glycine.[5] These toxic effects were, however, observed only when a millimolar concentration of glycine was applied, whereas the peak level of extracellular glycine during ischemia was in the micromolar range.[6] In contrast, high extracellular glycine failed to potentiate NMDA-evoked depolarization in vivo.[7] Glycine protected neurons from hypoxia-induced toxicity in cortical neuron cultures.[8] Recently, several antagonists at the glycine site of the NMDA receptor have been developed, and their neuro-

Received November 6, 2006; accepted January 22, 2007.

From the Division of Neurosurgery (M.O., T. Sugawara, S.M., T.O., K.M., H.K.), Department of Neuro and Locomotor Science, Akita University School of Medicine, Akita; the Department of Medical Genetics (S.K., K.K., T. Shinka, K.S., A.N., Y.A., Y.M.), Tohoku University School of Medicine, Sendai; and the Department of Neurosurgery (H.K.), Faculty of Medicine, University of Yamanashi, Tamaho, Yamanashi Japan.

Correspondence to Shigeo Kure, MD, Department of Medical Genetics, Tohoku University School of Medicine, 1-1 Seiryomachi, Aobaku, 980-8574, Japan. E-mail skure@mail.tains.tohoku.ac.jp

Stroke is available at http://www.strokeaha.org

DOI: 10.1161/STROKEAHA.106.477026

protective effect was reported in experimental stroke.[9] Based on these in vitro effects of glycine and the in vivo effects of antagonists for the NMDA receptor glycine site, it has been repeatedly suggested that glycine may contribute to the development of ischemic injury.[10] To the best of our knowledge, however, no direct evidence has been provided for the in vivo effect of extracellular glycine concentrations on ischemic injury. It is probably because there is no set of experimental animals that have distinct concentrations of extracellular glycine.

Glycine is released from the presynaptic membrane to the synaptic cleft and then either transferred into presynaptic neurons or transported into astrocytes through glycine-specific transporters.[11] In astrocytes, the glycine cleavage system (GCS) degrades glycine efficiently and generates the concentration gradient between the cytosol and extracellular space,[11–13] which enables glycine transporters to transfer glycine from the synaptic cleft into the astrocyte. The distribution of the GCS is inversely related to local glycine levels in the brain,[12] indicating its importance in determination of basal glycine concentrations. The GCS is a mitochondrial enzyme complex with 4 individual components: glycine decarboxylase (GLDC), aminomethyl transferase, aminomethyl carrier protein, and lipoamide dehydrogenase.[14] GLDC is a homodimeric enzyme of ≈200 kDa. An inherited deficiency of either GLDC or aminomethyl transferase causes an inborn error of metabolism, glycine encephalopathy (GE), also called nonketotic hyperglycinemia.[15] GE is characterized by neonatal coma and convulsions associated with the accumulation of large amounts of glycine in cerebrospinal fluid, providing further evidence that the GCS plays a fundamental role in maintaining extracellular glycine concentrations in the central nervous system.

To clarify the role of extracellular glycine in brain ischemia, we examined neuronal injury after transient occlusion of the middle cerebral artery (MCA) in mice with altered GCS activities by monitoring extracellular amino acid concentrations. Mice with altered GCS activities were generated by transgenic expression of normal GLDC or a dominant-negative mutant of GLDC, which was previously found in a family with GE[16] and characterized in this study. These approaches have enabled us for the first time to elucidate a direct correlation between extracellular glycine concentrations and ischemic injury.

Materials and Methods

Expression Analysis of GLDC cDNA in COS7 Cells

We previously identified a 3-base deletion, c.2266 to 2268delTTC, in the *GLDC* gene in a GE family, which resulted in the deletion of 1 phenylalanine residue at amino acid position 756, delF756.[16] The mother was a heterozygous carrier of the 3-base deletion and had a serum glycine level 1.8-hold higher than normal, which is considered the upper limit of the normal range. This observation prompted us to test whether the delF756 mutation had a dominant-negative effect. A 3.7-kb DNA fragment encoding human GLDC cDNA was subcloned into a pCAG vector (P-wild) for expression analysis (Figure 1A). The pCAG vector was kindly provided by Prof Jun-ichi Miyazaki of Osaka University (Osaka, Japan).[17] Mutant GLDC cDNA with the delF756 mutation was also subcloned into pCAG (P-delF756). The pCAG vector containing β-galactosidase cDNA was prepared as a negative control. Plasmid DNAs of the pCAG vector, P-wild, P-delF756, and β-galactosidase were purified with a plasmid purification midi kit (Qiagen GmbH, Hilden, Germany). Preparation of COS7 cells, transfection with lipofectamine (Invitrogen Corp, Carlsbad, Calif), cell harvest, and assay of GLDC enzymatic activity were performed as described.[16]

Generation of Transgenic Mouse Lines

P-wild and P-delF756 plasmids were digested with *SalI*, and a 5.4-kb DNA fragment was recovered (Figure 1A). After purification of the DNA fragments, they were injected into fertilized eggs of BDF1 mice for generation of transgenic mice. Genomic DNA was purified from mouse tails with use of a DNeasy tissue kit (Qiagen), and a 201-bp DNA fragment of the CAG promoter region was amplified by polymerase chain reaction with a pair of primers, RBGP-1 and -2, for identification of the transgene. Nucleotide sequences of the primers were as follows: for RBGP-1, 5′-GCCCCTTGAGCATCTG ACTTCTGG-3′ and for RBGP-2, 5′-GACCTCTTTATAGCCACCTT TG-3′. We mated the founder mice with C57BL/6 strain mice to obtain F_1 mice and screened for cerebral glycine concentration. Transgenic mice of 2 selected lines, high-GCS and low-GCS mice, were backcrossed with C57BL/6 mice 10 times and used for the following studies.

Enzymatic Analysis of GLDC and GCS Activity

GLDC enzymatic activity was determined by an exchange reaction between CO_2 and glycine with $NaH[^{14}C]O_3$ as described.[16] GCS activity was measured by a decarboxylation reaction with [1-^{14}C]glycine as described.[13]

Regional Cerebral Blood Flow Measurement

Regional cerebral blood flow was measured by the laser-Doppler flowmeter method with a Laserflo BPM2 (Vasamedics, St. Paul, Minn). The flowprobe (0.5-mm diameter) was placed on the cranial bone above the MCA territory (0.5 mm posterior and 4 mm lateral from the bregma) and away from large surface vessels. Steady-state baseline values were recorded before MCA occlusion, and blood flow data were then expressed as percentages of preocclusion baseline. No significant difference in the percent change in cerebral blood flow values was detected during and after ischemia (supplemental Figure I, available online at http://stroke.ahajournals.org).

Induction of Focal Cerebral Ischemia

Males of high-GCS, low-GCS, and control C57BL/6 mouse lines weighing 25 to 30 g were used for the ischemia study. Anesthesia was induced with 2% halothane in a closed chamber and maintained with 1.0% to 1.5% halothane in 30% O_2 and 70% N_2O delivered via facemask. Rectal temperature was monitored and maintained at 37±0.5°C with a thermal blanket throughout the surgical procedure. Focal cerebral ischemia was induced by MCA occlusion by the intraluminal suture technique.[18] A 5–0 nylon monofilament suture with a round tip was inserted into the internal carotid artery 11±0.5 mm from the bifurcation of the common carotid artery until the laser-Doppler flowmeter signal abruptly dropped. After 60 minutes of MCA occlusion, the nylon suture was removed and blood flow restoration was confirmed by the laser-Doppler flowmeter signal. Mice in which the laser-Doppler flowmeter signal during ischemia exceeded 10% of the preischemic signal were excluded from this study. All experiments and surgical procedures were approved by the Akita University Animal Care and Use Committee.

In Vivo Microdialysis

Twenty-four hours before MCA occlusion, vertical microdialysis probes (0.22-mm outer diameter, 2-mm membrane length; Eicom Corp, Tokyo, Japan) were stereotaxically implanted in the left striatum of mice under anesthesia. The probe was coordinately implanted at 0.6 mm anterior and 2.0 mm lateral to the bregma and 2 mm ventral from the brain surface, according to the 1997 atlas of Franklin and Paxinos. The external portions of the probes were fixed to the skull with dental cement. Throughout ischemia, dialysis probes were perfused with Ringer's solution (147 mmol/L NaCl,

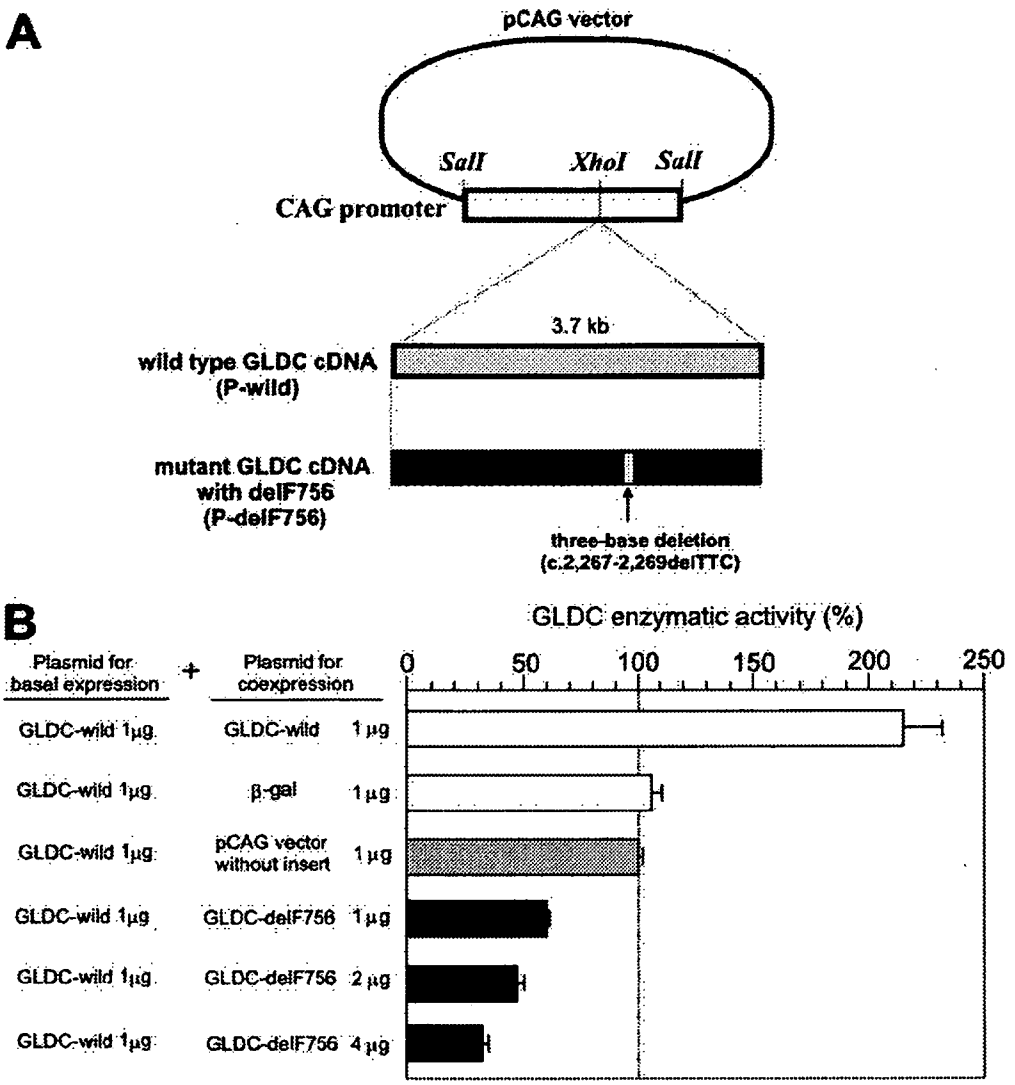

Figure 1. Expression analysis of GLDC cDNA in COS7 cells. A, Construct of expression vectors. Normal human GLDC cDNA (≈3.7 kb) was inserted into the *Xho*I site of the pCAG plasmid (P-wild). A mutant GLDC cDNA with the 3-base deletion, c.2266 to 2268delTTC, was similarly inserted into the pCAG plasmid (P-delF756). B, Coexpression study of P-wild and P-delF756 expression plasmids in COS7 cells. One microgram of P-wild plasmid, together with various other plasmids, was transfected into COS7 cells. The GLDC activity of COS7 cells transfected with 1 μg P-wild plasmid and 1 μg pCAG plasmid was defined as 100%, and relative GLDC activity (%) is shown. Note that less GLDC activity was observed when more P-delF756 plasmid was transfected with the fixed amount of P-wild plasmid.

2.3 mmol/L $CaCl_2$, 4.0 mmol/L KCl; pH 7.0) at a rate of 2 μL/min. The microdialysate (20 μL) was collected every 10 minutes. After a stabilization period of 1 hour, the samples were collected from 1 hour before MCA occlusion to 2 hours after MCA occlusion. Amino acid concentrations in the samples were measured by high-performance liquid chromatography (Eicom Corp).

Administration of SM-31900

An inhibitor of the glycine binding site of the NMDA receptor, SM-31900 (Sumitomo Pharmaceuticals Co Ltd, Osaka, Japan), was dissolved in physiological saline, which was then adjusted to pH 8.5.[19] The animals subjected to MCA occlusion were randomly assigned to vehicle or SM-31900 treatment groups. Vehicle or SM-31900 (10 mg/kg IV) was administered twice at 30 and 10 minutes before MCA occlusion.

Measurement of Infarct Size and Infarct Volume

Twenty-four hours after MCA occlusion, the mice were deeply anesthetized and decapitated. The brain was removed and sectioned coronally into four 2-mm slices with a mouse brain matrix (Harvard Apparatus, Cambridge, Mass). The slices then were placed in 2% 2,3,5-triphenyltetrazolium chloride solution at 37°C for 10 minutes and fixed in a 10% buffered formalin solution. The infarct area, stained white, was measured with NIH Image analysis software, and infarct volume was calculated by summing the infarct volumes of sequential 2-mm-thick sections.[20] Infarct volume was measured in different groups of animals from those used for microdialysis studies because infarct volume cannot be evaluated after probe insertion for microdialysis.

Statistics

All data were expressed as mean±SD. The statistical differences in regional cerebral blood flow and amino acid concentrations among and within the mouse groups were analyzed by a 1-way ANOVA and Dunnetts's test for multiple comparisons. Significance was accepted with $P<0.05$.

Results

Identification of Dominant-Negative GLDC

When 1 μg of plasmid with normal human GLDC cDNA (P-wild) was expressed in COS7 cells, the specific GLDC

activity was 9.8±0.8 nmol of glycine formed per milligram protein per hour, which was defined as 100% GLDC activity (Figure 1B). Expression of 2 μg of P-wild plasmid resulted in 215.8±19% GLDC activity. Negligible GLDC activity was detected in transfection of 1 μg of P-delF756 plasmid.[16] GLDC activity was reduced to 62.1±0.3%, 47.0±1.9%, and 32.0±1.6% in cotransfection with 1, 2, and 4 μg P-delF756 plasmid together with 1 μg P-wild plasmid, respectively (Figure 1B). No reduction in GLDC activity was observed when 1 μg β-galactosidase plasmid was cotransfected. Because GLDC activity was inhibited in response to amounts of P-delF756, we concluded that the delF756 mutation had a dominant-negative effect.

Generation and Biochemical Characterization of the High-GCS Mouse Line

Normal GLDC cDNA and mutant GLDC cDNA with the delF756 mutation were subjected to transgenic expression in mice under control of the CAG promoter (Figure 1A). A *SalI*/*SalI* fragment (5.4 kb) of P-wild plasmid containing normal human GLDC cDNA was injected into 50 fertilized eggs. A total of 13 mice were born. One of them turned out to carry the transgene. It grew normally and was fertile to establish a transgenic mouse line. Mice of this line had significantly lower cerebral glycine concentrations (0.71±0.06 μmol/g wet tissue) than did wild-type C57BL/6 mice (0.90±0.05) as shown in Figure 2A. The enzymatic activity of the GCS was determined by a glycine decarboxylation reaction in tissue samples of mouse cerebrum. GCS activity was 0.48±0.14 nmol of CO_2 formed per milligram protein per hour, which was 340% of that of wild-type C57BL/6 mice (0.14±0.03). This transgenic mouse line was designated high GCS.

Generation and Biochemical Characterization of the Low-GCS Mouse Line

A *SalI*/*SalI* fragment (5.4 kb) of the P-delF756 plasmid containing mutant human GLDC cDNA (Figure 1A) was injected into 225 fertilized eggs, and 72 mice were born. The transgene was identified in 15 of 72 mice. By 3 months of age, 5 of 15 founder mice had died of unknown causes. We observed that 1 of those 5 mice exhibited shivering and loss of body weight at 3 month of age. Measurement of amino acid contents in the brain sample from that mouse showed a marked increase in glycine content, 3.2 nmol/g tissue in the cortex. We assumed that founder mice with massive glycine accumulations died at an early age, whereas founder mice with no or moderate glycine accumulations survived. The remaining 10 founder mice grew normally and were fertile. These founder mice were mated with wild-type C57BL/6 mice, and their F_1 offspring were screened for brain glycine content. The mouse line with the highest glycine content had 1.36±0.06 μmol glycine per gram of tissue in the cerebral cortex (Figure 2A), in which glycine content in the striatum was also significantly high (Figure 2B). GCS activity in the mouse cerebrum was 0.04±0.01 nmol of CO_2 formed per milligram protein per hour, which was 29% of that of control C57BL/6 mice (0.14±0.03). This mouse line was designated low GCS. Histological examination revealed no abnormality in either high-GCS or low-GCS mice (data not shown).

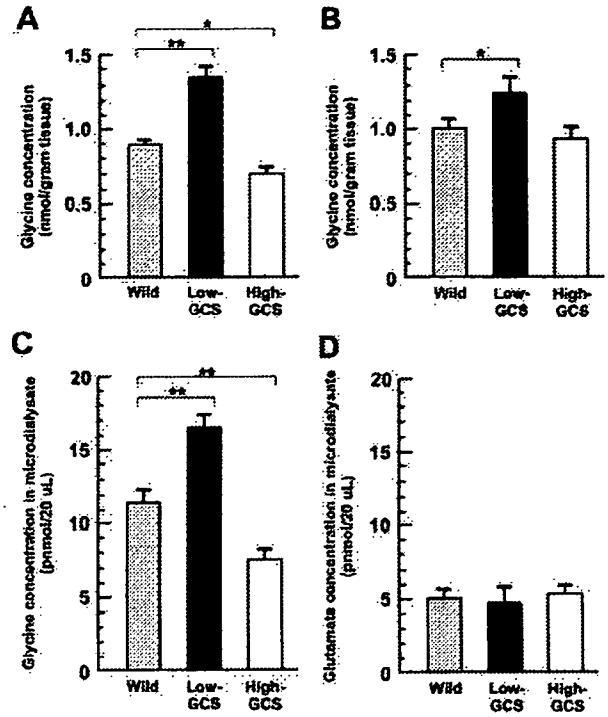

Figure 2. Glycine concentrations in high-GCS, low-GCS, and control C57BL/6 mice. Glycine contents in homogenate samples from the cerebral cortex (A) and striatum (B) were measured in the 3 mouse groups (n=6–8). Extracellular glycine (C) and glutamate (D) concentrations were analyzed by an in vivo microdialysis method. The extracellular glycine concentration was significantly higher ($P<0.01$) in low-GCS mice and significantly lower ($P<0.01$) in high-GCS mice compared with controls, whereas the extracellular glutamate concentration was not significantly different among the 3 mouse lines. *$P<0.05$, **$P<0.01$.

Basal Concentrations of Extracellular Amino Acid Neurotransmitters

Glycine concentrations in microdialysates were 11.7±1.0, 7.3±0.9, and 16.6±1.0 pmol/20 μL in wild-type C57BL/6, high-GCS, and low-GCS mice, respectively (Figure 2C). Extracellular glycine concentrations were therefore estimated as 1.0±0.1, 1.4±0.1, and 0.6±0.1 μmol/L in wild-type, low-GCS, and high-GCS mice, respectively, based on the sampling efficiency of our microdialysis system. Glutamate concentrations in microdialysates of wild-type C57BL/6, high-GCS, and low-GCS mice were 5.0±0.8, 5.4±0.7, and 4.8±1.5 pmol/20 μL, respectively (Figure 2D), which corresponded to 0.4±0.1, 0.5±0.1, 0.4±0.1 μmol/L, respectively, in extracellular glutamate concentration. The glycine and glutamate concentrations in wild-type mice showed good agreement with those in a previous report.[6] The extracellular concentration of glycine was significantly ($P<0.01$) higher or lower in low-GCS or high-GCS mice, respectively, compared with wild-type mice. No significant difference was observed among the 3 mouse lines in terms of extracellular concentrations of glutamate, taurine, alanine, or γ-aminobutyric acid (GABA), as shown in Figures 3C through 3E.

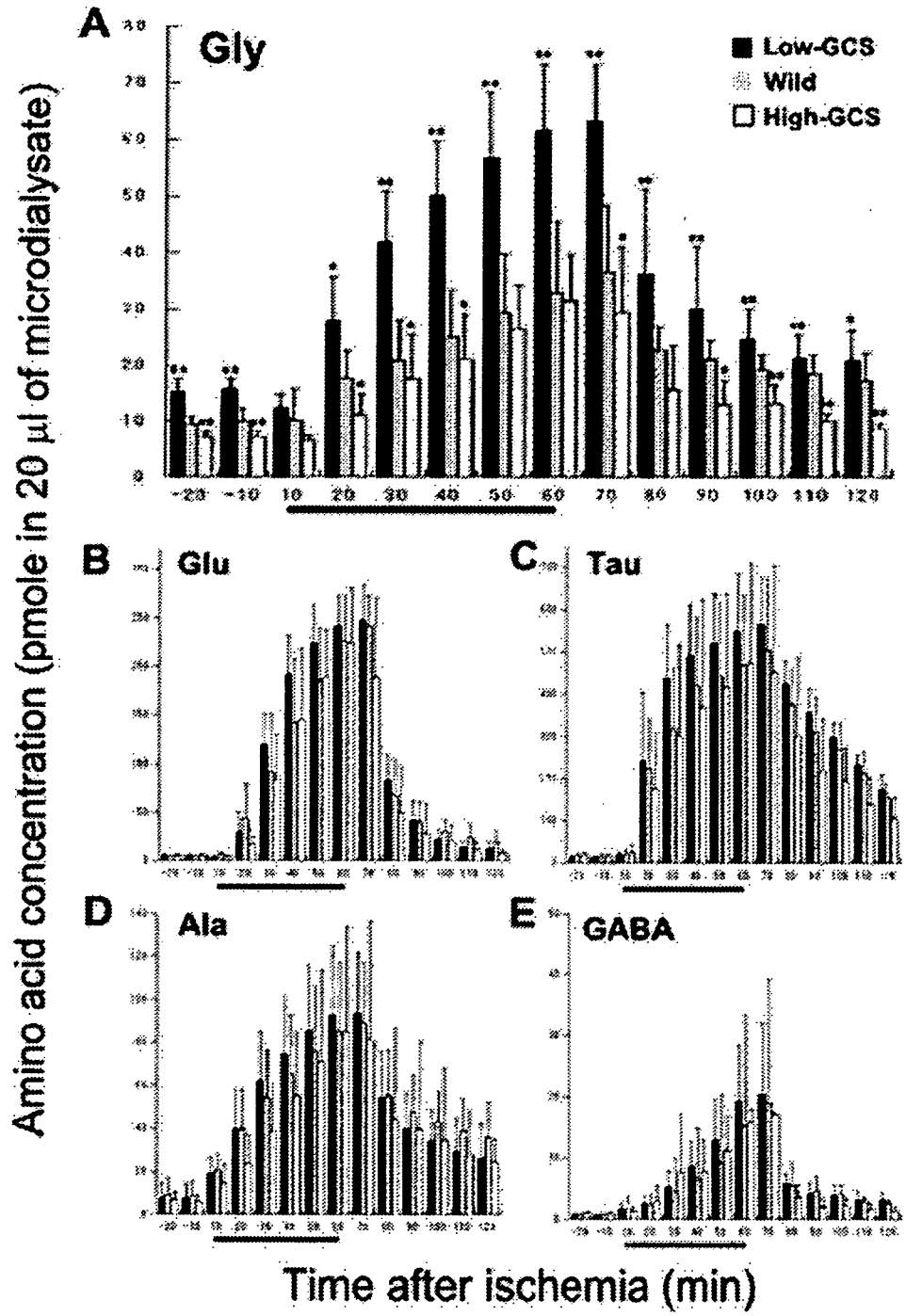

Figure 3. Extracellular concentrations of amino acid neurotransmitters in focal ischemia. A, The glycine concentration was significantly higher and lower in the low-GCS (n=10) and high-GCS (n=10) group, respectively, compared with controls (n=10). There were no significant differences in extracellular concentrations of glutamate (B), taurine (C), alanine (D), or GABA (E) among the 3 groups. The horizontal bar stands for the MCA occlusion period (60 minutes). Values are mean±SD. *$P<0.05$, **$P<0.01$.

Profiles of Extracellular Amino Acid Concentrations in MCA Occlusion

The glycine concentrations in all groups increased significantly at 20 minutes after MCA occlusion and reached their peak at 10 minutes after reperfusion (Figure 3A). The peak concentrations were 63.4±10.0, 36.6±12.0, and 31.5±7.9 pmol/20 μL in low-GCS, C57BL/6, and high-GCS mice, respectively. During and after MCA occlusion, glycine concentrations were persistently higher in low-GCS mice and lower in high-GCS mice compared with control mice. The glutamate concentrations were elevated in all 3 groups at 20 minutes after MCA occlusion and eventually reached their peak (247.7±35.9, 241.2±31.0, and 165.41±92.0 pmol/20 μL in low-GCS, C57BL/6, and high-GCS mice, respectively) at 10 minutes after reperfusion (Figure 3B). No significant difference in glutamate concentration was observed among the 3 groups

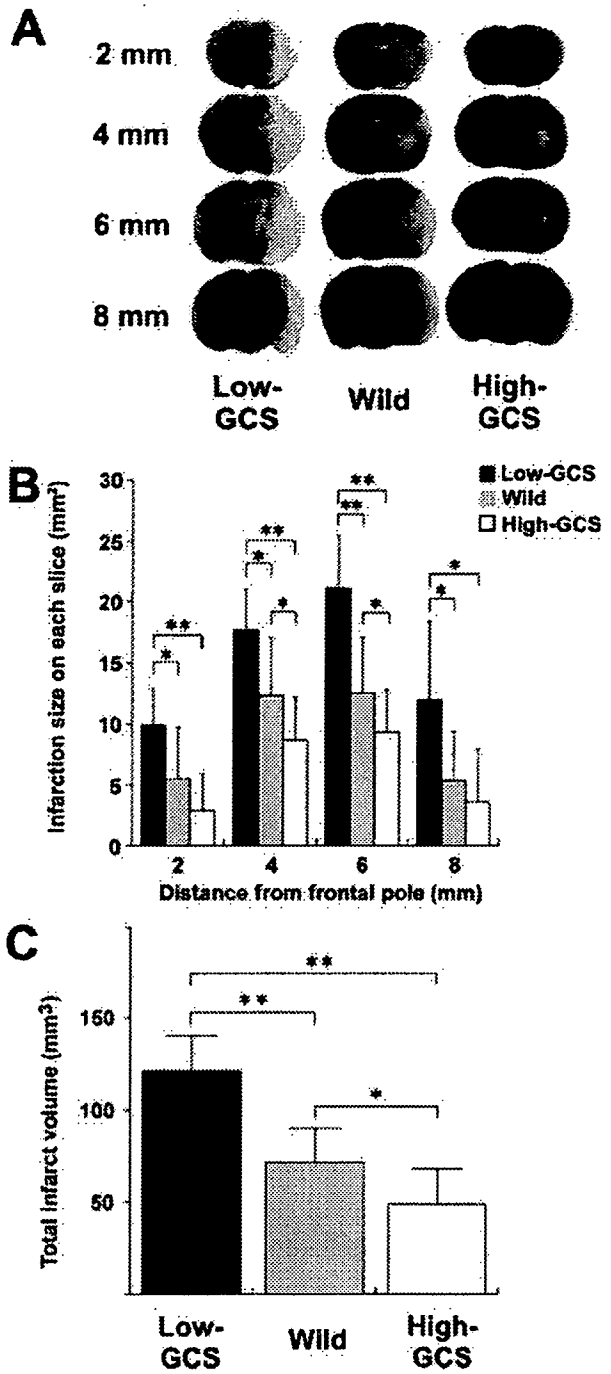

Figure 4. Evaluation of brain injury after MCA occlusion in low-GCS, high-GCS, and control C57BL mice. A 2-mm slice of brain sample was stained with triphenyltetrazolium chloride for visualization of the infarct region (white). Representative photographs of each mouse group (n=10) are shown (A). Infarct area (in mm^2) in each slice was measured (B). C, The infarct volume (in mm^3) in low-GCS mice was 69.8% larger than that of control mice. The infarct volume in high-GCS mice was 46.4% smaller than that of controls. Values are mean±SD. *$P<0.05$, **$P<0.01$.

throughout the experiments. MCA occlusion caused significant elevations of extracellular concentrations of taurine, alanine, and GABA (Figures 3C through 3E). There were no significant differences in extracellular taurine, alanine, or GABA concentrations among 3 mouse groups at each time point.

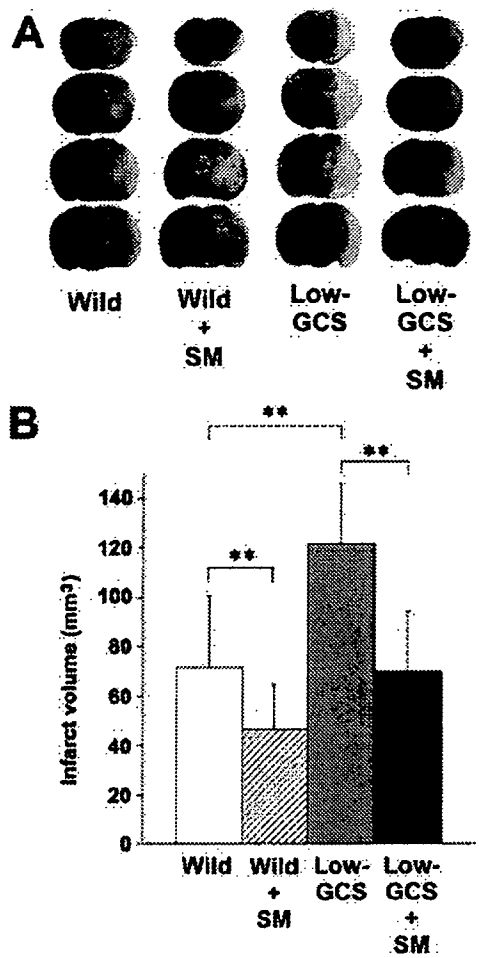

Figure 5. Effect of an NMDA receptor glycine site antagonist on cerebral infarction. Vehicle or SM-31900 (SM; 10 mg/kg IV) was administered twice at 30 and 10 minutes to wild-type C57BL/6 and low-GCS mice before MCA occlusion. A, Coronal brain slices were prepared from each mouse and then stained with triphenyltetrazolium chloride. B, Infarct volume was significantly reduced by SM-31900 administration in the control mice and more markedly in low-GCS mice. Mean±SD of each mouse group (n=6) is shown. **$P<0.01$.

Infarct Size

In C57BL/6 control mice, infarct areas were mainly in the cortex and striatum (Figure 4A). The infarct areas extended to the whole MCA territory in low-GCS mice, whereas the areas were confined to the striatum in high-GCS mice. The infarct area in low-GCS mice was significantly larger than that of control mice in all slices, whereas the area of 4- and 6-mm slices was significantly smaller in high-GCS mice compared with controls (Figure 4B). As shown in Figure 4C, infarct volume in low-GCS mice after MCA occlusion was significantly increased by 69%, and that in high-GCS mice was significantly reduced by 21% compared with wild-type mice (low-GCS mice, 121.6±19.0 mm^3; control C57BL/6 mice, 71.6±29.1 mm^3; high-GCS mice, 56.5±7.9 mm^3).

Effect of the NMDA Receptor Glycine Site Antagonist SM-31900 on Infarct Size

Compared with vehicle-treated mice, infarct regions in the striatum and cortex were smaller in the SM-31900–treated